J Membrane Biol (2015) 248:407–417
DOI 10.1007/s00232-015-9808-7

Peptide Folding in Translocon-Like Pores

Martin B. Ulmschneider[1] · Julia Koehler Leman[2] · Hayden Fennell[1] · Oliver Beckstein[3]

Received: 26 January 2015 / Accepted: 5 May 2015 / Published online: 28 May 2015

Abstract The cellular translocon, present in all three domains of life, is one of the most versatile and important biological nanopores. This complex molecular apparatus is directly responsible for the secretion of globular proteins across membranes as well as the insertion of integral membrane proteins into lipid bilayers. Recently determined structures of the archaean SecY translocon reveal an hour-glass-shaped pore, which accommodates the nascent peptide chain during translocation. While these structures provide important insights into ribosome binding to the translocon, threading of the nascent chain into the channel, and lateral gate opening for releasing the folded helical peptide into the membrane bilayer, the exact folding pathway of the peptide inside the protein-conducting channel during translocation and prior to the lateral release into the bilayer remains elusive. In the present study, we use molecular dynamics simulations to investigate atomic resolution peptide folding in hour-glass-shaped pore models that are based on the SecY translocon channel structure. The theoretical setup allows systematic variation of key determinants of folding, in particular the degree of confinement of the peptide and the hydration level of the pore. A 27-residue hydrophobic peptide was studied that is preferentially inserted into membranes by the translocon. Our results show that both pore diameter as well as channel hydration are important determinants for folding efficiency and helical stability of the peptide, therefore providing important insights into translocon gating and lateral peptide partitioning.

Keywords Protein folding · SecY translocon · Membrane protein · Molecular dynamics · OPLS

✉ Martin B. Ulmschneider
mulmsch1@jhu.edu; martin@ulmschneider.com

[1] Department of Materials Science and Engineering, Johns Hopkins University, Baltimore, MD 21218, USA

[2] Department of Chemical and Biomolecular Engineering, Johns Hopkins University, Baltimore, MD 21218, USA

[3] Center for Biological Physics and Department of Physics, Arizona State University, Tempe, AZ 85287, USA

Introduction

Most membrane proteins are integrated into cellular membranes via the translocon apparatus, which is a central part of a large protein network. Recently determined structures describe the translocon as a hetero-trimeric channel with an hour glass-shaped channel at its center, through which a nascent peptide chain is threaded when it arrives from the ribosome (Van den Berg et al. 2004). The translocon has a dual function: both transporting soluble protein chains destined for secretion across the membrane (Rapoport 2007), while also inserting hydrophobic segments of membrane proteins into the bilayer. This is achieved through the clam-shell-like structure formed by the N- and C-terminal halves of the channel, which have been proposed to open laterally toward the membrane (Park et al. 2014). The lumenal side of the protein also displays a small helical domain called the plug, which swings out during translocation (Gumbart and Schulten 2006, 2007) and is believed to block ion flow through the pore when no peptide chain is present in the channel (Rapoport 2007).

How the translocon decides whether a specific polypeptide segment should be integrated into the membrane rather than translocated across it is not conclusively known. However, several recently determined structures have provided important insights into translocon function. The

CryoEM structure of the laterally open conformation in nanodiscs at 7 Å resolution combined with molecular dynamics simulations have indicated the involvement of the cytosolic loops in signal peptide recognition (Frauenfeld et al. 2011). Specifically, the loop between transmembrane helices 6 and 7 likely undergoes large conformational changes, guiding the nascent peptide chain into the channel.

This view is supported by recently determined CryoEM structures of both the laterally open and closed form of the protein with the ribosome present (Park et al. 2014; Voorhees et al. 2014). The closed channel structure has an empty cytoplasmic funnel with the plug domain occupying the extracellular funnel. The nascent chain forms a loop on the cytoplasmic surface before entering the channel. On the extracellular side another loop connects the nascent peptide chain with the hydrophobic signal sequence, which forms a helix at the lateral gate. It is believed that the translocon continually opens and closes its lateral gate, exposing consecutive segments of the nascent peptide chain to the hydrophobic membrane interior (White and von Heijne 2008). While polar segments will prefer to remain inside the channel, resulting in their translocation across the membrane, sufficiently hydrophobic peptides are thought to partition into the lipid bilayer as helices one-by-one (Cymer et al. 2014). Recently, pulling forces between the individual transmembrane helices have been measured that are dependent on mutations in the helices and loop length between them (Cymer and von Heijne 2013). This general view on membrane insertion is supported by the fact that partitioning of both naturally occurring (Ulmschneider et al. 2006b), as well as designed transmembrane helices (Hessa et al. 2005) strongly correlates with their expected transfer free energies calculated from hydrophobicity scales (Hessa et al. 2007).

How much folding (if any) actually occurs inside the translocon channel is currently not known. It is clear from energetic estimates that partitioning of the unfolded peptide is highly unfavorable, largely due to the energetic penalty from unsatisfied backbone hydrogen bonds that would occur when moving an exposed peptide backbone from a semi-aqueous channel environment into a hydrophobic membrane interior (White and Wimley 1999). Furthermore, fully extended peptide segments would likely aggregate or misfold in the hydrophobic environment of the lipid bilayer. Partially or fully folded lateral release, therefore, seems more likely from an energetic and efficiency point of view. This belief is supported by experimental work on the folding of helix B in bacteriorhodopsin that found the transition state to be largely helical (Curnow and Booth 2009).

Even though the recent structures have provided a more detailed understanding of the translocon mechanism, it remains unclear what influence the channel dielectric environment and the pore diameter have on folding of the nascent peptide chain inside the channel. Computer simulations can provide valuable insights, since they model interactions at the atomic level to a good approximation, and can therefore contribute important information on how a structure will react to pore widening or narrowing. Molecular dynamics simulations of SecY in lipid bilayers have investigated channel gating (Haider et al. 2006), and pore widening by forcing a peptide through the central cavity (Gumbart and Schulten 2006, 2007). A recent coarse-grained molecular dynamics study in the nanosecond to minute timescale investigated efficiency of insertion versus translocation and suggests that pore confinement and the hydrophobic character of the pore are features regulating the translocon machinery (Zhang and Miller 2012b). Recent PMF calculations of peptides within the translocon channel have also demonstrated that both the spatial confinement and surface properties of the channel greatly favor helical conformations (Gumbart et al. 2011), which suggests that the channel itself might be play a role in the formation of TM helices. Interestingly, the spatial confinement of the pore seems to be stabilized by the plug domain, as found by molecular dynamics simulations (Gumbart and Schulten 2008).

Further, non-equilibrium all-atom simulations of the nascent chain growth in the nanosecond range with subsequent microsecond trajectories have shed light into protein insertion, docking of the signal peptide to the lateral gate, conformational changes of the translocon helices during folding, and partial release of the protein sequences into the membrane (Zhang and Miller 2012a). Interestingly, findings suggest that the orientation of the inserted protein is regulated by either salt-bridges between the N-terminus of the nascent protein, cytosolic loop residues, and phospholipid head groups that favor a $N_{cytosol}$ orientation, or hydrophobic contacts between the folding protein and the membrane bilayer that favor a N_{lumen} orientation. All-atom molecular dynamics simulations on the microsecond timescale also suggest a motion of the nascent chain between the open lateral gate and the membrane lipids, depending on the hydrophobicity of the peptide (Gumbart et al. 2013). Even for a closed gate, it seems that lipids can partially contact the nascent helix, which is also dependent on the hydrophobicity of the helix. These findings implicate that direct protein–lipid interactions at the lateral gate regulate transmembrane helix insertion into the bilayer and therefore helix release from the translocon.

The aim of the present study is to investigate to what degree and on what timescale peptide folding is possible inside the translocon channel. To achieve this, we use a theoretical pore model that approximates the shape and dimensions of the primarily hydrophobic SecY pore with a channel of methane-like particles that are held in place by

harmonic restraints. While this seems like a crude approximation at first, this model has several advantages: (1) It allows the effect of specific features of the pore to be studied and varied individually, providing an excellent tool for theoretical investigation of the channel properties, which can not be easily achieved using a full-atom model of a realistic SecY channel. (2) The very large size and complexity of the SecY translocon and associated machinery poses severe challenges to direct folding simulations, chiefly due to the prohibitive computational cost required to achieve timescales on which folding is likely to occur inside the channel (>μs), if indeed any folding occurs at all. (3) It simplifies the problem to few observables without the complexities of many interacting chains, large conformational changes and other influencing factors.

Our simplified theoretical channel model captures the key features of the SecY crystal structures with regards to channel hydrophobicity, and the diameter of the central pore (see Fig. 1). Using this model, we study the atomic resolution intra-translocon folding of a hydrophobic peptide, which was shown to preferentially insert into the membrane in an assay using the translocon machinery (Hessa et al. 2005). This insertion process is investigated with a modified version of the methane pore translocon channel that includes an open lateral gate with access to a lipid bilayer membrane (Fig. 1).

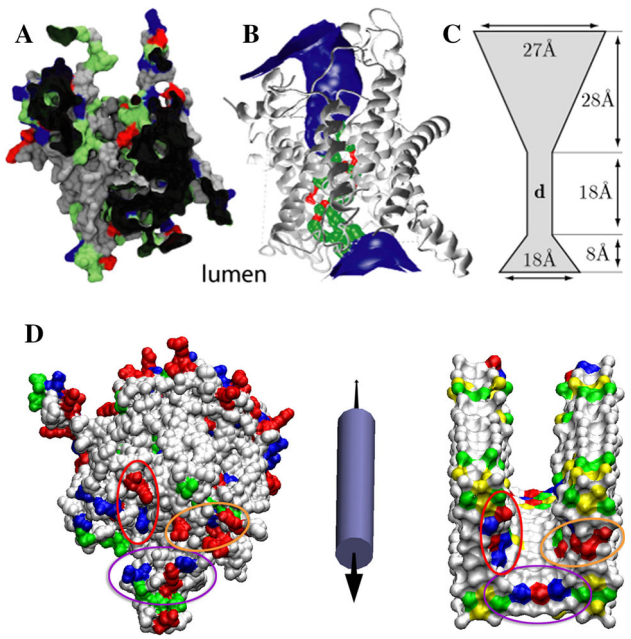

Fig. 1 The protein-conducting channel of the SecY translocon. **a** Cross-section through the 'closed' state channel of the SecY crystal structure (PDB code: 3DIN) (Zimmer et al. 2008). The colors indicate hydrophobic (*gray*), polar (*green*) and charged residues (*red*, *blue*). The pore is largely lined with hydrophobic residues. **b** Pore diameter profile (Smart et al. 1996) of the channel (PDB code: 1RHZ) (Van den Berg et al. 2004). **c** The equivalent channel topology used in the present simulations, which was modeled using united-atom methane spheres. The central pore diameter *d* was chosen to vary between 8 and 12 Å. The cytoplasmic side has the wider and longer cone (*upside*). **d** Front-view visualization of the surface polarity of 1RHZ.pdb and the modeled pore 10Pmap. Perspectives are skewed as shown in *center* (Color figure online)

It is estimated that the ribosome elongates the polypeptide chain at about 5 residues per second (Hershey 1991) and peptide folding typically occurs several orders of magnitude faster on the nano- to microsecond timescale. Since the translocon itself is thought to release the peptide into the membrane at a rate slower than elongation (Cheng and Gilmore 2006), the peptide segments would in principle have ample time to fold, provided sufficient space is available. Since we are investigating a hydrophobic peptide, we can safely neglect recently observed pulling forces from positive or negative charges in the protein sequence (Ismail et al. 2015), as well as peptide elongation and energetically driven movement along the channel pore. We furthermore assume that the translocon structure is locked into a well-defined state (i.e. open to the protein, lateral gate closed) for the duration of the simulations.

Folding of globular proteins under confinement has previously been studied using theoretical, coarse-grained, and atomistic models with differing results and conclusions depending on the system and model used (Lucent et al. 2007; Ojeda et al. 2009; Sorin and Pande 2006; Takagi et al. 2003; Zhou and Dill 2001; Ziv et al. 2005). Of particular interest for this study are simulations of peptide folding in carbon nanotubes. Theoretical predictions based on polymer models suggest that with decreasing pore diameter the confinement imposed by the nanotube will increase peptide helicity (Zhou and Dill 2001). In contrast to these considerations and to previous models, which treated the solvent with a mean-field approach, recent atomistic simulations of helix-forming peptides in aqueous solution show that explicit inclusion of water molecules leads to a stabilization of unfolded states at smaller pore diameters (Lucent et al. 2007; Sorin and Pande 2006). To reconcile these seemingly contradicting theories and observations, several fundamental differences should be taken into account: (1) the range of pore diameters considered (15–35 Å) is much larger than the putative translocon pore diameter and hence the peptide remains essentially inside an aqueous environment; here we investigate diameters ranging from 8 to 12 Å, which mirror the strong confinement experienced by the peptide during translocation. (2) Previous studies have concentrated on peptides that form helices in water, while peptides destined for membrane insertion generally form helices only in hydrophobic environments. (3) Peptides inside the translocon channel are in a very low-dielectric environment of the hydrophobic channel lining and the surrounding lipid bilayer environment at times when the channel is laterally open. In

contrast, in the carbon nanotube simulations, the tube is immersed in water. Thus, the peptide is likely to interact with water inside the tube via long-range Coulomb interactions, and will therefore experience a different electrostatic environment than in the translocon.

Methods

Modeling the Closed Protein-Conducting Channel

Hydrophobic hour-glass-shaped nanopores were modeled on the protein-conducting channel of the recent SecY crystal structures (Van den Berg et al. 2004; Zimmer et al. 2008). A pore diameter profile of the 'closed' SecY (i.e. lateral gate closed, open towards solution) reveals a narrow central channel with a length of $\sim$18 Å (PDB code: 1RHZ). Two large cone-shaped vestibules on either side extend the channel significantly beyond the hydrophobic core of the bilayer (see Fig. 1b). The cone facing the cytoplasm is much wider and longer than its counterpart on the lumenal side. A cross-section through the channel reveals that it is lined mainly by hydrophobic residues (see Fig. 1a).

The key geometrical features of the pore were reproduced using united-atom methane spheres (see Fig. 1c) (Beckstein and Sansom 2004). The channel was widened at the narrowest part to permit peptide insertion. Three different diameters were chosen: 8, 10, and 12 Å. The 8 Å constriction is too small to allow a helical peptide to be inserted, while the 10 Å pore can in principle accommodate a tightly fitting helix. The 12 Å pore can theoretically hold beta-strands, helices, as well as a select number of compact unfolded segments. This pore is embedded in a slab of methane spheres mimicking a membrane (see Fig. 1). The methane molecules are uncharged with $\sigma = 3.9$ Å. Each methane sphere was held in place near its initial position by a harmonic restraining force of 40 kcal mol^{-1} Å^{-1}.

Hydrophilic pores were generated by introducing four dipoles parallel to the plane of the membrane into the cytoplasmic funnel of the translocon pore. Partial charges were placed on adjacent methane molecules to model a dipolar moment of $\sim 2 \times 10^{-29}$ Cm, roughly equivalent to a fully exposed peptide backbone.

The peptide was inserted inside the pore in an extended conformation and no structural restraints were applied.

Modeling the Observed Pore Polarity

Additional simulations were performed using a 10 Å diameter pore that maps the translocon channel's polarity. This model uses both partially (i.e., $q < \pm 1$e) and fully charged (i.e., $q = \pm 1$e) methane spheres to approximate the positions and influence of charged and polar residues within the pore. Positive and negative residues were represented with single methane spheres with $q = \pm 1$e, while polar residues were represented by immediately adjacent pairs of partially charged spheres. A comparison between the real and model channel is shown in Fig. 1. The color-coded encircled regions illustrate the approximate polarity matching between the two channels.

Modeling the Laterally Open Protein-Conducting Channel

Simulations of the translocon pore with a laterally open gate and inserted peptide were modeled using identical methods. Columns of methane spheres were removed from the front of the pore to create a lateral gate with an opening of $\sim$10 Å. The aim was to allow a typical α-helix with a diameter of 10–12 Å to pass out of the channel into the bilayer. The width matches the estimated 8–16 Å width of the opening found in the translocon structures.

A POPC lipid bilayer was added at the open side of the channel and stabilized by groups of partially charged methane spheres added to the outside of the channel at the approximate height of the polar lipid head-groups. Additional groups of partially charged spheres were added to the top and bottom corners of the channel, as well as on the inside walls of the gate opening to reduce the hydrophobicity of the protein surface (Fig. 1). The system was solvated and the protein was allowed to fold freely within the channel starting from a fully extended conformation. No restraints or biasing potentials were applied.

Simulations

Simulations were performed using Gromacs version 4.0/4.6 (www.gromacs.org) (Hess et al. 2008) and hippo beta (www.biowerkzeug.com). The OPLS all-atom force field (Jorgensen et al. 1996) was used for the protein in combination with united-atom parameters for the methane pore and the TIP3P water model (Jorgensen et al. 1983). Long-range interactions were treated with a cut-off of 14 Å and bonds between heavy and hydrogen atoms were constrained using LINCS/RATTLE (Andersen 1983; Hess et al. 1997). Molecular dynamics simulations were run with a 2 fs integration time-step and neighbor lists were updated every 5 steps. Peptide, pore, and water were each coupled separately to a heat bath with a slightly elevated temperature of $T = 325$ K (=52 °C) to speed up sampling and a time constant of $\tau_T = 0.1$ ps using weak temperature coupling. Atmospheric pressure of 1 bar was maintained using weak pressure coupling with compressibility $\kappa_z = 4.6 \times 10^{-5}$ bar^{-1} and time constant $\tau_P = 1$ ps in the z-direction and fixed box dimensions in x and y (Berendsen et al. 1984).

Open pore systems were equilibrated at 55 °C and simulated at 120 °C for one microsecond to overcome kinetic energy barriers associated with lateral partitioning into the lipid bilayer. The stability of the peptide against thermal denaturing even at highly elevated temperatures has been previously demonstrated (Ulmschneider et al. 2010).

Simulations using the implicit membrane method were carried out using all-atom Metropolis Monte Carlo sampling with the same force field and temperature. The method has been described in detail in previous publications (Ulmschneider et al. 2007). In brief, the membrane is represented implicitly as a hydrophobic zone that becomes increasingly inaccessible to aqueous solvent, which is also modeled implicitly using the generalized Born theory of solvation. The implicit membrane approach allows vast increases in computational performance and has been successfully employed in a wide number of ab initio folding simulations, while the equivalence of the Monte Carlo sampling to molecular dynamics has been demonstrated (Ulmschneider et al. 2006a).

Results

Choice of Peptide

The 4L peptide (Sequence: Ace-GGPG-AAAALA-LAAAAALALAAAA-GPGG-Ame) from the 'biological hydrophobicity scale' developed by von Heijne and White was chosen for the present folding simulations. It represents a suitably simple test system and is inserted into membranes via the similar mammalian Sec61 translocon at high efficiency; the measured insertion probability is ~76 %, corresponding to an apparent insertion free energy of −0.64 kcal/mol (Hessa et al. 2005). As in the experimental setup, GGPG 'helix breakers' were added to the 4L sequence at either end. The termini were acetylated (Ace-) and amidated (-Ame), respectively.

Unconfined Peptide Folding in Membranes and Water

Before investigating peptide folding under the confinement of a translocon-like pore the folding without confinement in aqueous and membrane environments was investigated to determine the suitability of the hydrophobic 4L model peptide for the study. First, a generalized Born implicit membrane (GBIM) environment (Ulmschneider et al. 2007) was used to show that the 4L peptide follows the folding and insertion process postulated for membrane proteins (Jacobs and White 1989; Popot and Engelman 1990). 4L follows the folding-insertion pathway previously observed for hydrophobic peptides such as polyleucine and WALP: rapid membrane adsorption is followed by interfacial folding and subsequent stable helical insertion (see Fig. 2a, b) (Ulmschneider and Ulmschneider 2008a, b). The simulation independently verifies that 4L forms a stable transmembrane helix in an implicit membrane environment and is hence suitable for the present investigation. Repeating the simulation in a more realistic explicit atomic detail DPPC lipid bilayer confirmed the spontaneous peptide insertion pathway and demonstrated that the

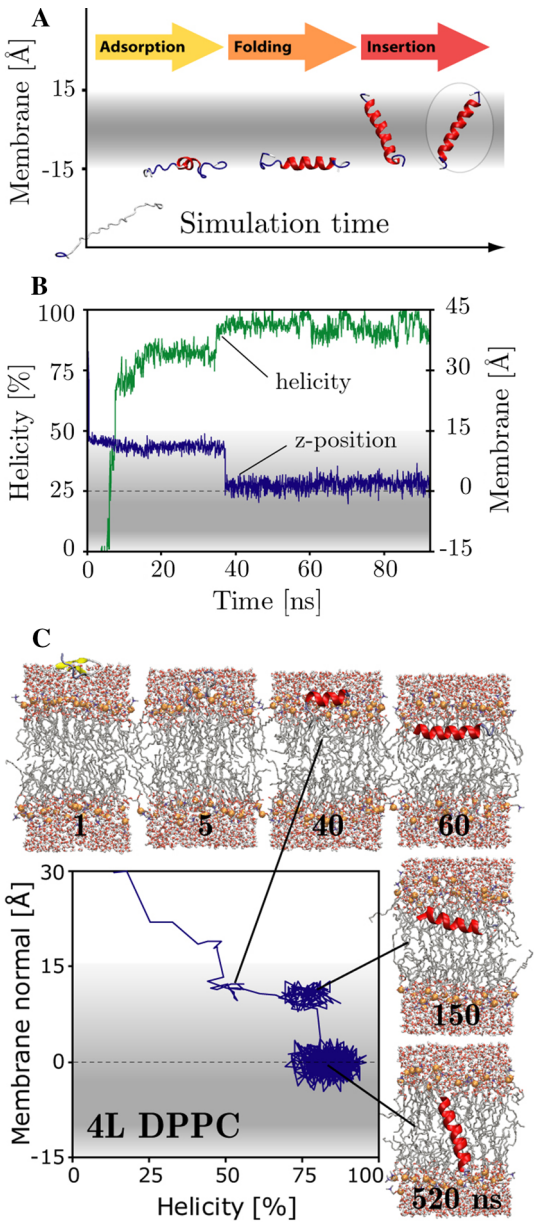

Fig. 2 Adsorption, interfacial folding and insertion of the 4L peptide in the implicit membrane (GBIM). **a** The folding pathway. **b** The peptide inserts shortly after fully folding. **c** Unbiased folding-partitioning of the 4L peptide in an atomic detail DPPC lipid bilayer membrane

native state is a stable transmembrane helix (see Fig. 2c). Both simulations show that the increased hydrophobicity at the membrane interface is sufficient to drive helical folding and that the fully folded helix is established within 50 ns. The insertion is much more rapid in the implicit model due to the absence of frictional terms.

In order to exclude the possibility that 4L forms stable helices in the absence of a membrane environment, a control simulation was performed in aqueous solution using the TIP3P water model. Indeed, the simulation showed that in water globular structures with low average helical content (less than 10 %) are the dominant conformations (Table 1), and helices are generally unfavorable. This demonstrates that any formation of helical secondary structure is not an intrinsic property of the peptide itself.

Table 1 gives a summary of all simulations performed in the present study. Each simulation was checked for full convergence. Key observables such as helicity and position along the pore were calculated as a function of simulation time. After 50 ns of simulation averages did not change substantially although the standard deviations decreased, indicating that our reported observables have converged within the timeframe of the simulations.

Folding in the Translocon Channel

Having established the suitability of the 4L peptide, simulations were carried out in simplified translocon-like channel pores of variable diameter. The overall channel geometry was taken from the SecY crystal structures (Van den Berg et al. 2004; Zimmer et al. 2008) and the central pore diameter was varied between 8 and 12 Å (see Fig. 1). For each diameter, both polar and fully hydrophobic pores were studied (see "Methods" section for details).

Figure 3 summarizes the folding behavior inside the hydrophobic (8H) and polar (8P) 8 Å diameter pores. Folding is severely restricted inside the narrow central part of the channel. For both pores, the simulations reveal that the 8 Å diameter is too small for helix formation, permitting only extended conformations. However, outside the central narrow part of the channel the peptide exhibits significant structural sampling. In the cytoplasmic funnel the dominant equilibrium conformation is helical, with the peptide adsorbed to the hydrophobic pore walls. In contrast, in the

Table 1 Simulations of the 4L biological scale peptide in a hydrophobic pore of variable central diameter (c.f. d in Fig. 1)

System	Diameter (Å)	Length (ns)	Helicity (%)	$t_{folding}$ (ns)
8H	8.0	100	65 ± 18	36
8P	8.0	100	16 ± 8	–
10H	10.0	200	48 ± 4	22
10P	10.0	200	54 ± 7	4
10N	10.0	100	24 ± 8	–
12H	12.0	100	12 ± 8	–
12P	12.0	100	60 ± 12	6
10Pmap	10.0	200	41 ± 7	–
10Popen	10.0	1000	58 ± 3	452
GBIM	–	90	93 ± 4	38
TIP3P	–	100	9 ± 6	–
DPPC	–	1000	84 ± 5	500

Both hydrophobic (H) and polar (P) pores were simulated, as well as a pore without any water (N). The helicity measures the percentage of the central 19 residues that are classified to be in helical conformation.(Ulmschneider et al. 2006a) It is averaged over the last 50 ns of each simulation. The total simulation time was >1 μs. $t_{folding}$ is the time it takes for the peptide to reach >50 % helicity for the first time. Control folding simulations were performed in an implicit membrane environment (GBIM) as well as water (TIP3P)

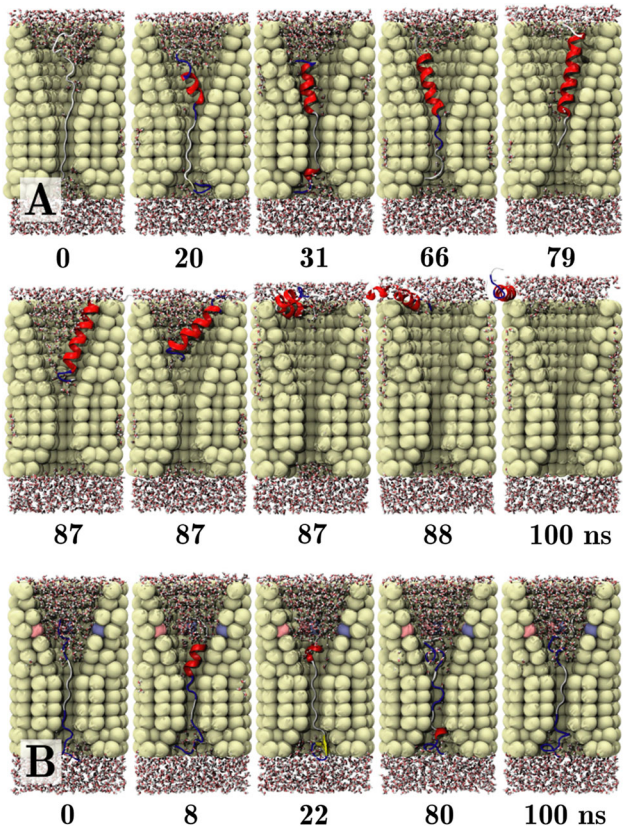

Fig. 3 Folding of the 4L peptide in the 8 Å diameter pore. **a** Folding in the narrow channel of the hydrophobic pore (8H) is restricted, since the central diameter is just too small to allow formation of a helix. Helix formation occurs rapidly in the cytoplasmic vestibule, with the helix (*red*) adsorbed to the hydrophobic pore walls. The N-terminal end is slowly dragged through the narrow central constriction leading to a fully folded helix in the vestibule. Entry of water causes the helix to be pulled to the rim of the cytoplasmic cone. By the end, the free energy minimum conformation is reached, with the helix adsorbed in a groove at the membrane–water interface. **b** In the polar pore (8P), the helix termini sample a broader range of secondary structures in the funnels. Helices are the dominant conformation, although turns and beta-strand-like structures are also transiently observed. Water solvates both funnels, in contrast to 8H (Color figure online)

lumenal vestibule the peptide segment remains largely unstructured, sampling a wide range of conformations, including small beta-strands and helices. The major difference between the polar and the hydrophobic pore is that the former contains water in both vestibules, irrespective of the presence of the peptide. The hydrophobic pore, however, is indeed too hydrophobic to be stably solvated and only when water molecules can condense around the polar peptide backbone will water enter the central regions of the cavity. Similar desolvation has been observed for the central cavity of the mechanosensitive MscS ion channel, which is also lined with hydrophobic residues and has a comparable pore diameter (Anishkin and Sukharev 2004), as well as other membrane channel proteins (Beckstein and Sansom 2003, 2004).

Decreased hydration in the hydrophobic pore leads to the N-terminal segment being slowly pulled through the central pore into the cytoplasmic vestibule. This process is accompanied by helical folding of each residue that emerges from the central channel, resulting in a fully folded helix in the vestibule, which is rapidly pulled out of the vestibule to the rim of the cytoplasmic cone by water molecules (Figs. 3a, 7a). From there it exits the pore adsorbing stably into a groove at the membrane–water interface. For the polar pore the hydration of the helix termini in the pore vestibules appears to create a sufficient barrier that holds the peptide pinned in the pore. Thus, the energetic cost of de-solvating the termini effectively prevents translocation of the peptide through the central, hydrophobic constriction, at least on the simulation timescales studied here.

Figure 4 shows that the slightly wider 10 Å pore generally permits the formation of a snugly fitting continuous membrane spanning helix inside the channel. The peptide segment inside the central cavity indeed rapidly forms a helix, which remains stable throughout the simulations, irrespective of pore hydrophobicity or level of hydration (c.f. 10H, 10P, 10N). While the hydrophobic pore (10H) expels most of the water from the cytoplasmic cavity, the polar pore model (10P) retains a fully solvated cavity, which results in a significantly decreased folding time and increased helical stability for the C-terminal peptide moiety in the cytoplasmic vestibule (see Table 1). Even in the complete absence of water (10N), the peptide still folds within the central narrow part of the pore (see Fig. 4c), although the termini rapidly unwind and reform helical structure. Water is important for the formation and stabilization of helical conformations at both peptide termini in the channel vestibules. Only the water-filled pore forms a helix with stably folded termini. Interestingly the simulation in vacuo (10N) also indicates that helix formation in the central cavity does not require water, and must therefore be a direct consequence of the severely restricted configurational space available to the peptide for sampling. Both 10H and 10P systems were extended for another

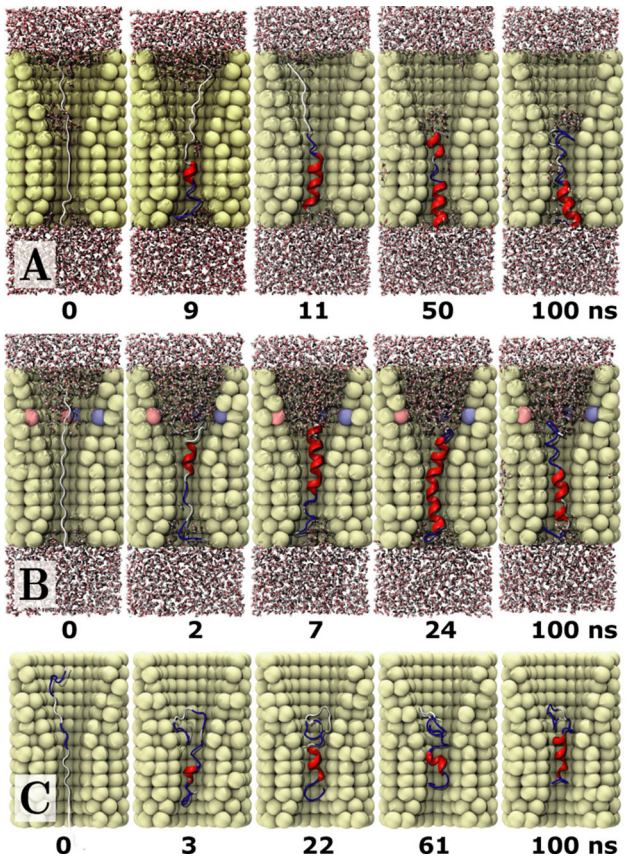

Fig. 4 Folding inside the 10 Å pore. **a** The hydrophobic pore (10H) expels the water from the larger cavity. **b** The polar pore model (10P) retains water and shows a similar folding pattern. **c** In the absence of water (10 N) the termini are destabilized. This simulations demonstrates that the helical formation in the central cavity of the channel is independent of water and a consequence of the severely restricted phase-space available to the peptide although solvation appears to protect the termini against unwinding

100 ns. The systems retain their conformations reached toward the second half of the first 100 ns simulation, demonstrating that they were already fully converged.

The 12 Å diameter pore in principle allows a much wider range of conformations to be sampled in the central part of the channel. Indeed, folding inside the hydrophobic (12H) pore shows rapid sampling of both helical and beta-hairpin conformations (see Fig. 5). However, in the absence of water the C-terminus is rapidly pulled through the central pore (c.f. 8H). Once in the lumenal cone, unfolded coiled conformations dominate and the peptide exits the channel occasionally. In the presence of water the folding pattern follows that which is observed for the smaller 10 Å pore. As with the 10 Å pore, helical formation occurs rapidly inside the central channel. The helix remains adsorbed to the hydrophobic pore walls. The free energy minimum conformation is rapidly reached and consists of a fully folded helix with termini solvated in the two vestibules.

Polarity Mapped and Open Pores

Folding within the polarized pore (10Pmap) exhibits similar behavior to the 10H, 10P, and 12P pores. Helix formation is fast within the hydrophobic central constriction and the termini remain solvated in the more polar vestibules. By 100 ns, the peptide has formed a stable central helix with solvated, unfolded termini. The peptide structure remains unchanged upon continuation of the simulation for an additional 100 ns, demonstrating that the system has converged. The data suggest that the peptide conformation within the translocon channel can be stabilized by the presence of water in the pore, as also seen in the 10P and 12P systems (Fig. 6).

Simulations of the open-gate model (10Popen) show rapid peptide folding, with initial helicity forming at ~20 ns. 50 % helicity of the peptide is reached at ~450 ns. After folding, the protein shifts laterally toward the opening of the gate, but remains within the pore for the entire duration of the 1-μs simulation. The peptide does not partition into the bilayer over the course of the simulation. This could be due to the increased hydrophobicity of the pore, which creates a pore environment that might be energetically preferable for the peptide. Alternatively, the gate might not be wide or flexible enough for the helix to partition. Further simulations with significantly increased timescales will be required to address these questions.

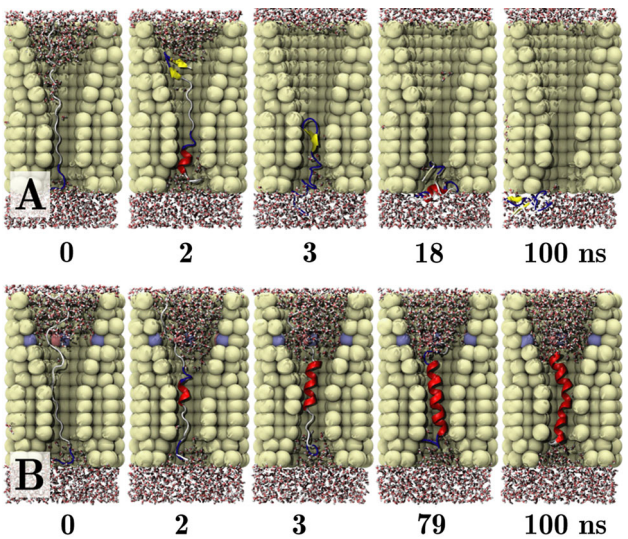

Fig. 5 Folding in the wider channel of the 12 Å pore occurs only in the presence of water in the lumenal vestibule. **a** In the absence of water the C-terminus is rapidly pulled through the central pore (hydrophobic 12H pore). Unfolded coiled conformations dominate and the peptide exits the lumenal cone occasionally. **b** In the presence of water helical formation occurs rapidly inside the central channel (polar 12P pore). The helix remains adsorbed to the hydrophobic pore walls of the central constriction. The global free energy minimum conformation is rapidly reached and consists of a fully folded helix with termini solvated in the two vestibules

Discussion

Folding in Pores

Compared to a membrane or aqueous folding environment the main effect of the pore is peptide confinement; enthalpic interactions of the peptide with the pore are small due to the hydrophobic character of the pore lining particles. The shape and diameter of the channel severely limit the conformational space accessible for the peptide to explore. In the central cylindrical cavity this restricts the peptide to elongated conformations. Since the alpha-helix has by far the lowest free energy in this conformational subspace, it should be the preferred conformation sampled. This is indeed observed in the present simulations, as long as the diameter of the pore is sufficiently wide to accommodate a helix. Fully extended unfolded conformations are unfavorable due to their higher energy and low entropy, while partially folded states of lower energy and higher entropy, which would dominate in an unconfined environment, are excluded due to the shape of the cavity.

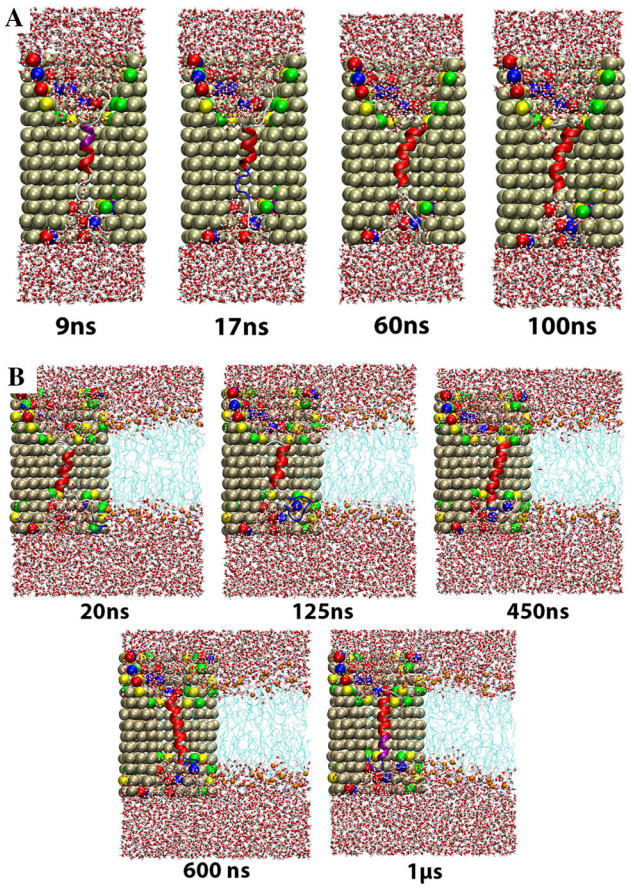

Fig. 6 **a** Folding in the polar closed pore. Speed of helix formation mirrors that of the 10P pore. **b** Cutaway view of folding in the open 10 Å pore. The helix favors the gate (*right*) side of the translocon once full helicity is reached (~450 ns)

Variation in the pore diameter results in slight variations of the accessible conformational space. For the 8 Å pore this limits the peptide to extended unfolded conformations, while the larger 12 Å pore was found to briefly sample beta-hairpins (see Fig. 5). Nevertheless, the helix remains the dominant conformation for channels wide enough to accommodate it.

Remarkably, pore diameter is more important for helical folding than hydration, as evident from the fact that folding is observed even in the absence of water (see Figs. 4, 7b). However, water molecules play a very important role in the funnels of the channel, where they catalyze folding and stabilize helical conformations (see Table 1). This is demonstrated by the decreased folding time and increased helical stability of the peptides in the polar pores, which retain fully solvated funnels (see Fig. 7). A second feature of hydration is that the peptide is effectively immobilized inside the channel, at least for the timescales of the simulations studied here. Figure 7a shows that the peptides inside the polar pores hardly move along the channel, while the movement inside the hydrophobic pores is much larger, resulting in the eventual exit of the peptide in two cases. The high mobility of peptides inside these narrow pores at low hydration levels is surprising, and is likely the result of asymmetric hydration in the funnels. Yet, all-atom simulations suggest that flexibility of the pore residues may influence hydration in the pore (Gumbart and Schulten 2008). Water molecules pushed out of the hydrophobic funnel will effectively pull the peptide with them (see Fig. 3a). This suggests that different levels of hydration along the pore might act as a tether to pull the peptide through the pore.

Lateral Partitioning

Simulations of the open-gate translocon model demonstrate rapid peptide folding within the protein-conduction channel. While the folded peptide moves from the central axis of the channel toward the open lateral gate no partitioning into the lipid bilayer is observed. This suggests the microsecond timescales of the simulations are too short to capture the partitioning process. At present, the timescales over which the lateral gate remains open are not known. Assuming that the peptide does indeed fold inside the translocon the pore, the present simulations suggest that the partitioning process is orders of magnitude slower than the folding time of the peptide in the pore, and that during translocon-mediated insertion the peptide is therefore in thermodynamic equilibrium between the translocon channel and the gate, which in turn will presumably be in thermodynamic equilibrium with the lipid bilayer.

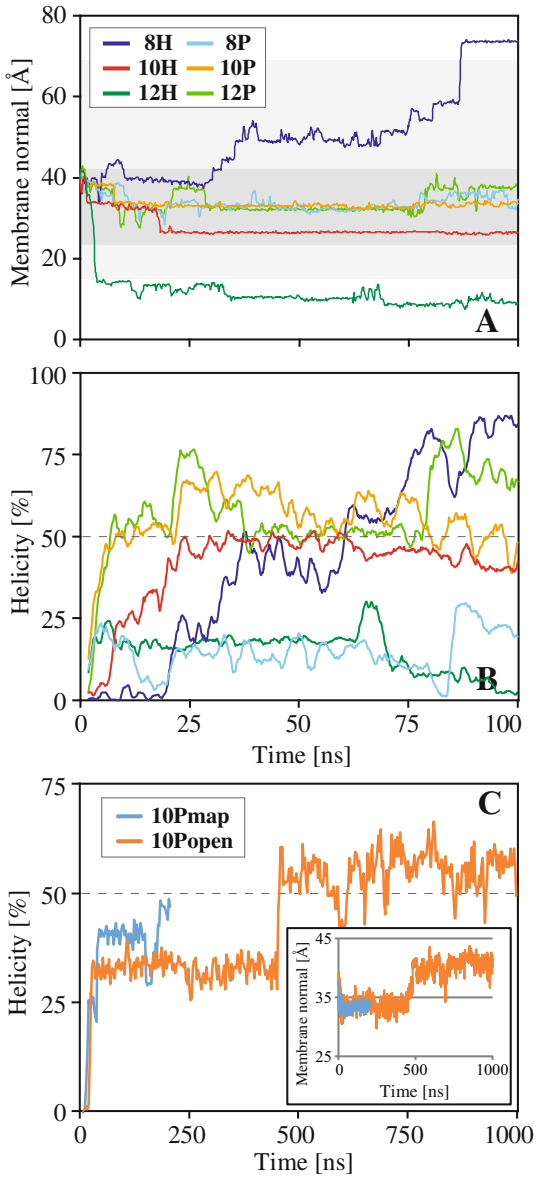

Fig. 7 **a** Position along the membrane normal (z-position) of the 4L peptide in the pore. The position of the membrane mimetic is indicated by the *gray area*, with the central constriction *shaded darkest*. **b** Helicity (see also Table 1 for the averages over the last 50 ns). All curves are running averages, to make them more accessible. The 10H and 10P simulations were continued for an additional 100 ns and showed stable helicities fluctuating around 48 and 54 %, respectively (data not shown). **c** Helicity and z-position (*inset*) values for 10Pmap and 10Popen. 10Pmap strays just beneath the 50 % helicity line while 10Popen spends the entire second half above 50 %—likely a result of the open gate allowing enough spatial freedom to counteract the solvation from increased polarity

Implication for Translocon Function

Even though the alpha-helix is the dominant conformation inside channels of suitable width, the strain displayed by the structures inside the channel (as indicated by the

comparatively low helicity and visible distortions) suggests that by leaving the confinement the peptides should be able to lower their free energy considerably. That such lateral partitioning of the confined helices into the membrane will indeed further relax the structure can be directly inferred from the implicit membrane simulation. Here both the overall helicity and structural stability are generally much larger, resulting in less strained and more 'relaxed' structures (c.f. the helicity and standard deviations in Table 1, and visually compare Fig. 2a with Figs. 4, 5b). The reason is the unconstrained conformational space of the peptide in the membrane, which is allowed to fold and reorient freely in space. This finding is important, since it suggests an explanation why helical segments will exit the translocon channel laterally into the membrane at high efficiency. It also provides a source of energy to drive SecY gating and lateral peptide partitioning.

The present computational study suggests that hydrophobic segments inside the translocon might fold completely or partially at the terminal ends, prior to their lateral release into the lipid bilayer. In the case of partially folded segments, only a few central helical turns need to form after release into the bilayer to produce a membrane spanning helix. Since this segment is in the most hydrophobic part of the bilayer this process will proceed downhill on the energy gradient, and would therefore be extremely rapid. Another aspect in favor of this folding model is that it explains how aggregation of unfolded peptide segments is prevented upon lateral release into the membrane. This is particularly relevant for multi-spanning membrane proteins, where it is difficult to conceive how unfolded chains released from the translocon could fold efficiently when pressed against previously released protein fragments.

A recent review of integral membrane protein behavior has proposed the idea that transmembrane segments may, in fact, not enter the central channel at all (Cymer et al. 2014). Rather, it is suggested that peptide segments make contact with the membrane interface near the translocon and are pulled directly through the lateral gate, skipping the pore entirely. In relation to our model this suggests two possibilities. Either the folding could take place in a laterally open gate, under some form of confinement defined by a half-open translocon gate and a lipid bilayer, or the folding could take place entirely on the protein-bilayer interface, suggesting that the translocon merely acts as a catalyst for transporting polar groups across the hydrophobic membrane.

Conclusions

Ab initio folding simulations from fully extended conformations show that pores that are too narrow to allow helices retain fully extended conformations inside the central cavity (diameter <10 Å), while wider pores (diameter ≥ 10 Å) allow rapid formation of stable helical structures. Channel hydration does not substantially affect folding within the narrow constriction of the channel, which remains free of water in all cases, likely due to the combination of its hydrophobic character with the spatial restriction. However, the interaction of water molecules with the peptide termini inside the funnels was found to catalyze helical formation on either side of the central cavity, therefore stabilizing the folded state and immobilizing the peptide in the pore. Although stable, the helices formed inside the cavity are heavily strained. Comparison with helices folded directly into a membrane environment suggests that the peptide can gain additional free energy through relaxation after its lateral release into the membrane bilayer. This might provide a driving force for translocon gating and lateral peptide partitioning.

Acknowledgments Images were prepared with VMD and rendered with Tachyon (Humphrey et al. 1996).

References

Andersen HC (1983) Rattle: a "velocity" version of the shake algorithm for molecular dynamics calculations. J Comput Phys 52:24–34

Anishkin A, Sukharev S (2004) Water dynamics and dewetting transitions in the small mechanosensitive channel MscS. Biophys J 86:2883–2895

Beckstein O, Sansom MSP (2003) Liquid-vapor oscillations of water in hydrophobic nanopores. Proc Natl Acad Sci USA 100:7063–7068

Beckstein O, Sansom MSP (2004) The influence of geometry, surface character, and flexibility on the permeation of ions and water through biological pores. Phys Biol 1:42–52

Berendsen HJC, Postma JPM, van Gunsteren WF, DiNola A, Haak JR (1984) Molecular dynamics with coupling to an external bath. J Chem Phys 81:3684–3690

Cheng Z, Gilmore R (2006) Slow translocon gating causes cytosolic exposure of transmembrane and lumenal domains during membrane protein integration. Nat Struct Mol Biol 13:930–936

Curnow P, Booth PJ (2009) The transition state for integral membrane protein folding. Proc Natl Acad Sci USA 106:773–778

Cymer F, von Heijne G (2013) Cotranslational folding of membrane proteins probed by arrest-peptide-mediated force measurements. Proc Natl Acad Sci USA 110:14640–14645

Cymer F, von Heijne G, White SH (2014) Mechanisms of integral membrane protein insertion and folding. J Mol Biol 427:999–1022

Frauenfeld J, Gumbart J, Sluis EO, Funes S, Gartmann M, Beatrix B, Mielke T, Berninghausen O, Becker T, Schulten K, Beckmann R (2011) Cryo-EM structure of the ribosome-SecYE complex in the membrane environment. Nat Struct Mol Biol 18:614–621

Gumbart J, Schulten K (2006) Molecular dynamics studies of the archaeal translocon. Biophys J 90:2356–2367

Gumbart J, Schulten K (2007) Structural determinants of lateral gate opening in the protein translocon. Biochemistry 46:11147–11157

Gumbart J, Schulten K (2008) The roles of pore ring and plug in the SecY protein-conducting channel. J Gen Physiol 132:709–719

Gumbart J, Chipot C, Schulten K (2011) Free-energy cost for translocon-assisted insertion of membrane proteins. Proc Natl Acad Sci USA 108:3596–3601

Gumbart JC, Teo I, Roux B, Schulten K (2013) Reconciling the roles of kinetic and thermodynamic factors in membrane-protein insertion. J Am Chem Soc 135:2291–2297

Haider S, Hall BA, Sansom MSP (2006) Simulations of a protein translocation pore: SecY. Biochemistry 45:13018–13024

Hershey JW (1991) Translational control in mammalian cells. Annu Rev Biochem 60:717–755

Hess B, Bekker H, Berendsen HJC, Fraaije JGEM (1997) LINCS: a linear constraint solver for molecular simulations. J Comput Chem 18:1463–1472

Hess B, Kutzner C, van der Spoel D, Lindahl E (2008) GROMACS 4: algorithms for highly efficient, load-balanced, and scalable molecular simulation. J Chem Theory Comput 4:435–447

Hessa T, Kim H, Bihlmaier K, Lundin C, Boekel J, Andersson H, Nilsson I, White SH, von Heijne G (2005) Recognition of transmembrane helices by the endoplasmic reticulum translocon. Nature 433:377–381

Hessa T, Meindl-Beinker NM, Bernsel A, Kim H, Sato Y, Lerch-Bader M, Nilsson I, White SH, von Heijne G (2007) Molecular code for transmembrane-helix recognition by the Sec61 translocon. Nature 450:1026–1030

Humphrey W, Dalke A, Schulten K (1996) VMD—visual molecular dynamics. J Mol Graph 14:33–38

Ismail N, Hedman R, Linden M, von Heijne G (2015) Charge-driven dynamics of nascent-chain movement through the SecYEG translocon. Nat Struct Mol Biol 22(2):145–149

Jacobs RE, White SH (1989) The nature of the hydrophobic binding of small peptides at the bilayer interface: implications for the insertion of transbilayer helices. Biochemistry 28:3421–3437

Jorgensen WL, Chandrasekhar J, Madura JD, Impey RW, Klein ML (1983) Comparison of simple potential functions for simulating liquid water. J Chem Phys 79:926–935

Jorgensen WL, Maxwell DS, Tirado-Rives J (1996) Development and testing of the OPLS all-atom force field on conformational energetics and properties of organic liquids. J Am Chem Soc 118: 11225–11236

Lucent D, Vishal V, Pande VS (2007) Protein folding under confinement: a role for solvent. Proc Natl Acad Sci USA 104:10430–10434

Ojeda PA, Londono A, Nan-Yow C, Garcia M (2009) Monte Carlo simulations of proteins in cages: influence of confinement on the stability of intermediate states. Biophys J 96:1076–1082

Park E, Menetret JF, Gumbart JC, Ludtke SJ, Li W, Whynot A, Rapoport TA, Akey CW (2014) Structure of the SecY channel during initiation of protein translocation. Nature 506:102–106

Popot JL, Engelman DM (1990) Membrane-protein folding and oligomerization—the 2-stage model. Biochemistry 29:4031–4037

Rapoport TA (2007) Protein translocation across the eukaryotic endoplasmic reticulum and bacterial plasma membranes. Nature 450:663–669

Smart OS, Neduvelil JG, Wang X, Wallace BA, Sansom MSP (1996) HOLE: a program for the analysis of the pore dimensions of ion channel structural models. J Mol Graph Model 14:354

Sorin EJ, Pande VS (2006) Nanotube confinement denatures protein helices. J Am Chem Soc 128:6316–6317

Takagi F, Koga N, Takada S (2003) How protein thermodynamics and folding mechanisms are altered by the chaperonin cage: molecular simulations. Proc Natl Acad Sci USA 100:11367–11372

Ulmschneider JP, Ulmschneider MB (2008a) Sampling efficiency in explicit and implicit membrane environments studied by peptide folding simulations. Proteins 75(3):586–597

Ulmschneider MB, Ulmschneider JP (2008b) Membrane adsorption, folding, insertion and translocation of synthetic trans-membrane peptides. Mol Membr Biol 25:245–257

Ulmschneider JP, Ulmschneider MB, Di Nola A (2006a) Monte Carlo vs molecular dynamics for all-atom polypeptide folding simulations. J Phys Chem B 110:16733–16742

Ulmschneider MB, Sansom MS, Di Nola A (2006b) Evaluating tilt angles of membrane-associated helices: comparison of computational and NMR techniques. Biophys J 90:1650–1660

Ulmschneider MB, Ulmschneider JP, Sansom MSP, Di Nola A (2007) A generalized born implicit membrane representation compared to experimental insertion free energies. Biophys J 92:2338–2349

Ulmschneider MB, Doux JPF, Killian JA, Smith J, Ulmschneider JP (2010) Mechanism and kinetics of peptide partitioning into membranes. J Am Chem Soc 132:3452–3460

Van den Berg B, Clemons WM Jr, Collinson I, Modis Y, Hartmann E, Harrison SC, Rapoport TA (2004) X-ray structure of a protein-conducting channel. Nature 427:36–44

Voorhees RM, Fernandez IS, Scheres SH, Hegde RS (2014) Structure of the mammalian ribosome-Sec61 complex to 3.4 A resolution. Cell 157:1632–1643

White SH, von Heijne G (2008) How translocons select transmembrane helices. Ann Rev Biophys 37:23–42

White SH, Wimley WC (1999) Membrane protein folding and stability: physical principles. Annu Rev Biophys Biomol Struct 28:319–365

Zhang B, Miller TF 3rd (2012a) Direct simulation of early-stage Sec-facilitated protein translocation. J Am Chem Soc 134:13700–13707

Zhang B, Miller TF 3rd (2012b) Long-timescale dynamics and regulation of Sec-facilitated protein translocation. Cell Rep 2:927–937

Zhou HX, Dill KA (2001) Stabilization of proteins in confined spaces. Biochemistry 40:11289–11293

Zimmer J, Nam Y, Rapoport TA (2008) Structure of a complex of the ATPase SecA and the protein-translocation channel. Nature 455: 936–943

Ziv G, Haran G, Thirumalai D (2005) Ribosome exit tunnel can entropically stabilize Î±-helices. Proc Natl Acad Sci USA 102: 18956–18961